

MAGNETIC FIELD MEASUREMENTS IN THE MSU 500 MEV SUPERCONDUCTING CYCLOTRON*

P. Miller, H. Blosser, D. Gossman, B. Jeltema, D. Johnson, P. Marchand
Cyclotron Laboratory, Michigan State University, East Lansing, Michigan 48824

Summary

The measurements of the magnetic field in the superconducting cyclotron under construction at Michigan State University are reported. The 55-channel flip coil gaussmeter built at MSU for this purpose is described. Twelve field maps measured with various currents in the two sections of the main coil have been Fourier-analyzed for evaluation of magnetic imperfections and data errors and for comparison with calculated magnetic field distributions. The calculation procedure is in excellent agreement with the measured data. The imperfection harmonics are small and there is evidence in the measurements that they are partly correctable by better alignment of pole tips and coil tank at final assembly of the cyclotron.

Apparatus

The gaussmeter uses 55 flip coil/integrator sets with computer controlled data scanning. The hardware is similar in concept to that developed to map the field of the Oak Ridge Cyclotron¹.

Moving parts are mostly non-metallic to reduce eddy current effects. The coils are wound on Delrin bobbins with an outer diameter of 3/8", and contain about 500 turns of #34 AWG enamelled copper wire (R=16Ω). They are mounted .5" apart in holes drilled in a 7/8" dia. rod made from G-10 epoxy-fiberglass material. The rod is rotated by strings connected to a non-magnetic air operated piston. The probe mechanism has to fit within the 1" magnet gap between pole liners. The azimuthal drive mechanism and the strings for rotation of the rod pass through the center hole in the magnetic yoke. Electrical wires are routed through another large hole in the yoke. The azimuthal scanning is done with a stepping motor coupled to a worm drive. The stepping motor requires a 3-layer cylindrical magnetic shield to keep it from stalling in the fringe field near the yoke at full magnet excitation. The entire apparatus works automatically under computer control through a complete field map.

The integrators consist of Analog Devices type 234L operational amplifiers with a feedback network time constant RC=0.022 sec. In the early design stages, temperature compensated ceramic capacitors seemed to be the best choice, and temperature regulation of the integrators was thought to be unnecessary. Further testing revealed that polystyrene capacitors, having negligible leakage and smaller dielectric polarization, would be a better choice in spite of their negative temperature coefficient of about 10⁻⁴/°C. The effect of a temperature change on the coils and the integrators has been measured, as described below. Due to procurement difficulties, two different size capacitors had to be used to complete the full array of integrators.

Five integrators are assembled in one NIM module. Eleven modules are therefore required. A Hewlett Packard 3490 A digital voltmeter scans through the integrators by means of a reed relay multiplexer (Matrix Corp. 1701). The measurement cycle for 55 integrators takes about 18 sec (relay setting time 100 msec plus measurement time of 230 msec per channel). The voltmeter is inherently insensitive to noise pickup at the power line frequency or its harmonics. The calibration constant for each channel was obtained by operating the apparatus in a uniform field measured with an NMR

*This material is based upon work supported by the National Science Foundation under Grant No. Phy 78-01684.

probe. Calibrations at 4 fields (1.5 to 13.5 kilo-gauss) confirm the integral linearity of the response to within 0.03%. If extrapolated linearly to 60 kilo-gauss this would produce a calibration error ≤ 0.14%.

The magnetic field B=kΔV is inferred as the product of the coil-integrator calibration constant k and the average integrator voltage change for two flips (one up and one down). Thus, a linear integrator drift is cancelled. (Typical integrator drift rate is 0.1 mV/sec.; the time between measurements before and after a flip is about 20 sec.). To correct for temperature changes one would multiply k by the factor

$$(1 + C_E \Delta T_E - C_C \Delta T_C),$$

where the last two terms refer to the coils and the electronics, and the ΔT's represent temperature changes relative to the temperature at the time the calibration constant k was determined. Average values of the experimentally measured coefficients are given in Table 1.

Table 1. Typical Fluxmeter Properties

Type	Integrator No.	C _C	C _E	avg. noise	avg. k
	Components of	(C-1)	(C-1)	(T)	±S.D. (T/V)
	units				
1	.022uf 1M	41	9x10 ⁻⁵	3x10 ⁻⁴	.9x10 ⁻⁴ .675±.020
2	.1 uf 220K	14	5x10 ⁻⁵	8x10 ⁻⁵	.6x10 ⁻⁴ .672±.021

The two types of integrator exhibit different average temperature coefficients. The coil temperature coefficients are found to lie between the thermal expansion predictions for the plastic coil form (2x10⁻⁴) and the copper conductor (3x10⁻⁵), as expected, since temperature induced variation of coil resistance is negligible. The temperature coefficient of the electronics operates with opposite sign from the anticipated one due to the capacitance change. We suspect that the temperature coefficient of the resistors is larger than expected, but this has not been verified.

Because the temperature fluctuations during mapping were small (≈1°C) the temperature corrections were not included in the computer program, although temperature data were recorded with the field maps automatically. The temperatures of the probe arm and three of the integrator modules are registered by four calibrated thermistors in series with a precision shunt and a d.c. power supply. The thermistor and shunt voltages are read by the computer every time the integrators are read.

Stability and Precision

A special computer program tests the repeatability and stability of the entire system. The computer repeatedly flips the measuring bar and stores the magnetic field measured by each integrator and the time on a file for later processing. The bar azimuth is not changed during the measurements. All 55 channels show a downward drift of the magnetic field of about 6 gauss in one hour, apparently the result of drift of the power supply current. This effect as well as any uniform temperature-induced drift is corrected during magnet mapping by normalizing the measurements to keep the central field constant.

The magnetic field history from each integrator is fitted to a second degree polynomial, since the drift rate is not uniform but can be seen to decrease with time in a plot of the data. The rms deviation of the

measurements with respect to the fitted function is the precision, which ranges from 0.5×10^{-4} T to 1.4×10^{-4} T. The average values for the two types of integrators are given in Table 1 under the heading "noise." The reason why certain integrators give consistently less noise than others is not known. Statistically, the type 2 integrators are slightly favored, but the spread within one type overlaps with the other.

Magnet Mapping Analysis

The main coil of the magnet is divided into two sections for coarse trimming of the radial field profile. The smaller section, which contains about 1/3 of the total number of turns, is closer to the midplane and therefore produces a field with a higher edge gradient than the large coil. Field maps were obtained with the two sections of the main coil excited to currents shown in Table 2.

Table 2. Main Coil Currents

Map. No.	Small Coil (A)	Large Coil (A)
1	498	498
2	400	400
3	600	600
4	700	700
5	200	200
8	400	400
10	600	700
11	700	600
12	700	400
13	700	200
14	400	200
15	600	400
16	400	600

The Fourier components for several maps were compared to those from a field distribution calculated by Blosser and Johnson². Some small discrepancies ($\approx 1\%$) in the average field profiles were traced to details of the iron distribution which were not included in the original calculation. The calculation itself was refined, as described below, to make the geometrical representation of the steel in the calculation more realistic. When these corrections were made the agreement was within 0.3% in the 700 A average field. The measured average field vs. radius is plotted in Fig. 1, and the deviation of the calculated field from the measurements is plotted in Fig. 2. Note that each radial position corresponds to one flip coil location. The peak structure that appears in all three sets of data is probably a measure of the relative calibration errors among individual flip coils ($\pm 0.03\%$). The vertical translation of the curves can be caused either by inaccuracy of the calculation or by a calibration error (e.g. gaussmeter temperature effect or power supply current).

The refined magnetic field calculations make use of the ability of the relaxation code to calculate with different magnetic permeability in different places. This allows the radial and axial boundaries of the steel to be entered accurately. The azimuthal structure is treated by scaling the magnetization to the fraction of the volume occupied by steel. This is implemented approximately, due to numerical limitations of the code, by dividing the steel into a few regions, each with a constant scale factor, as shown in Fig. 3.

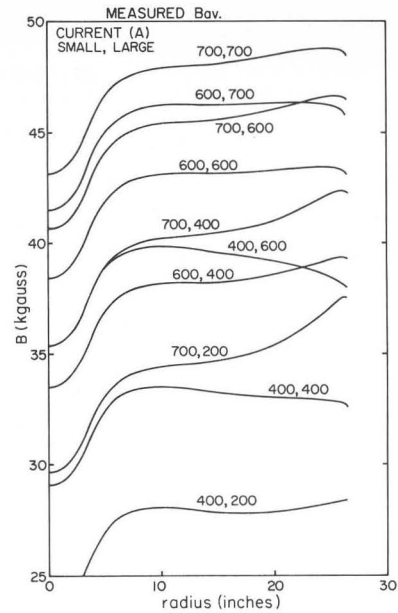


Fig. 1. Radial profile of the average magnetic field measured in the 500 MeV magnet for various combinations of currents in the two sections of the main coil.

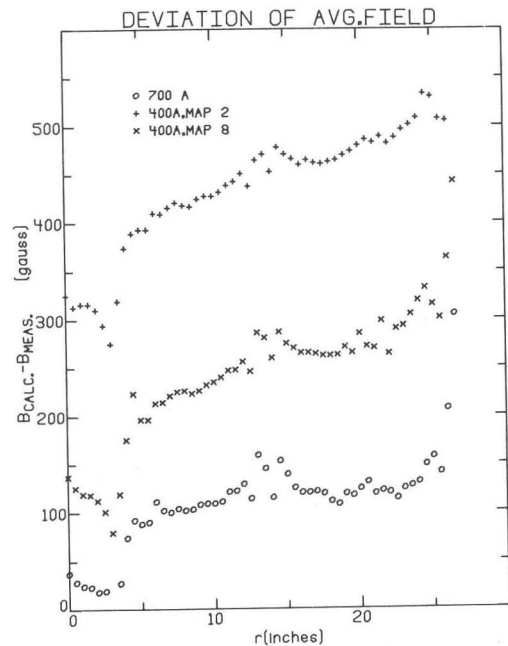


Fig. 2. Radial profile of the difference between the average field calculated by the procedure described in the text and the measured one.

Since the spaces in the iron do not have constant angular width, average scale factors are used. This approximation is corrected, however, by superposing the saturated iron field from the small regions ignored by this simplification, as well as the nonsymmetric parts due to the actual holes and spaces in the steel, as described in ref. 2.

The third harmonic amplitude B_3 in the 700 A measured field was within 5% of the calculation and the sixth harmonic differed by 7 to 15 % from its corresponding value. In the 200 A map, where the average field is about 2.2T, B_3 is still within 7% of the calculated (saturated iron) profile. The overall agreement between calculation and measurement implies that detailed orbit calculations can be carried out in

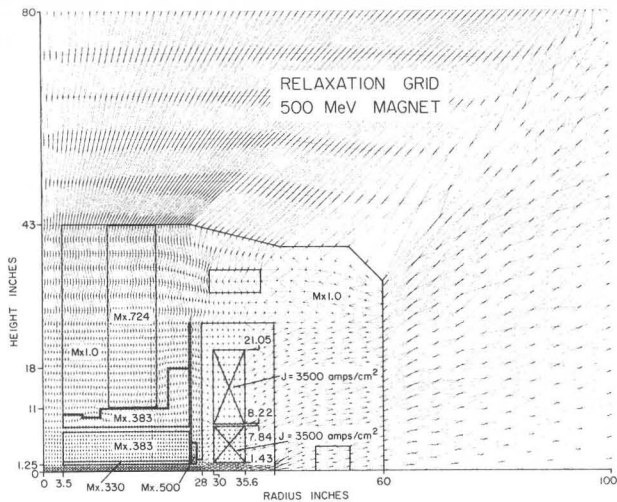


Fig. 3. Grid used in the relaxation calculation of the circularly symmetric portion of magnetic field. The magnetization M inferred from the B vs. H curve for 1020 steel is multiplied by different normalization factors in different areas to represent the fraction of the volume occupied by iron.

fields generated from the calculation procedure. This avoids the common difficulties associated with smoothing and interpolating in measured field maps.

Evaluation of Magnet Imperfections

The first and second harmonic components of the measured fields were found to be small, and they pose no difficulties for operation of the cyclotron. These Fourier components were partly a result of noise, drift, etc. of either the measuring apparatus or the magnet power supply and are partly true components of the magnetic field, due to deviation from ideal symmetry in the magnet structure.

The first harmonic is the most important imperfection because the orbit center is sensitive to this component at the crossing of the $\nu = 1$ resonance. The amplitude B_1 is shown in Fig. 4 as a fraction of the average field, which is the parameter of relevance for beam effects.

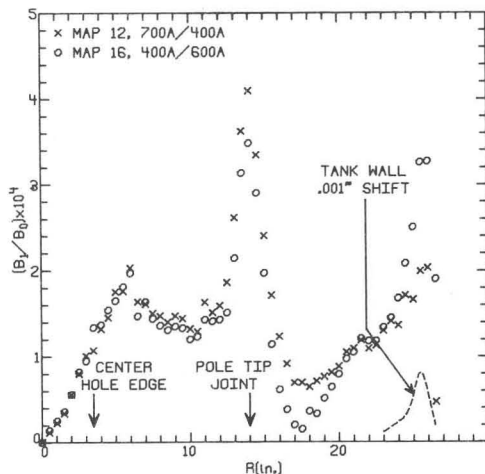


Fig. 4. Radial profile of the first harmonic amplitude B_1 expressed as a fraction of the average field B_0 for two typical maps. The calculated curve giving the effect of a .001 inch centering error of the coil was normalized for an average field of 4.08 Tesla. A centering error of about .003 inch is implied by the data.

A large peak near $r=14$ inches, where there is a joint in the pole pieces, indicates a misalignment of these parts. Some mechanical difficulties were noticed when the pole tips were installed, but rather than wait for construction of the redesigned spacers, the assembly was finished with the available parts. We expect that the problem can be corrected when the pole tips are removed to install the trim coils.

A smaller peak which has a shape and location resembling that inferred from the coil tank field gradient is presumably due to a centering error of that structure. The amplitude of the first harmonic is proportional to the centering error. There is some indication in these data of a shift in the coil tank position between the times the two maps shown were measured. It is even possible that the shift is induced by the change in current distribution in the two coil sections.

The consistency and smoothness of the phase angle is a good indicator of true field components. In Fig. 5 we show the amplitude and phase of both the first and the second harmonics for the same two maps as in Fig. 4. The repeatability of these independent measurements implies that the harmonics are in the field and are measured accurately. The peak in B_2 near $r=26$ inches is expected, since the coil tank has a machining error which makes it out-of-round by 0.030 inch.

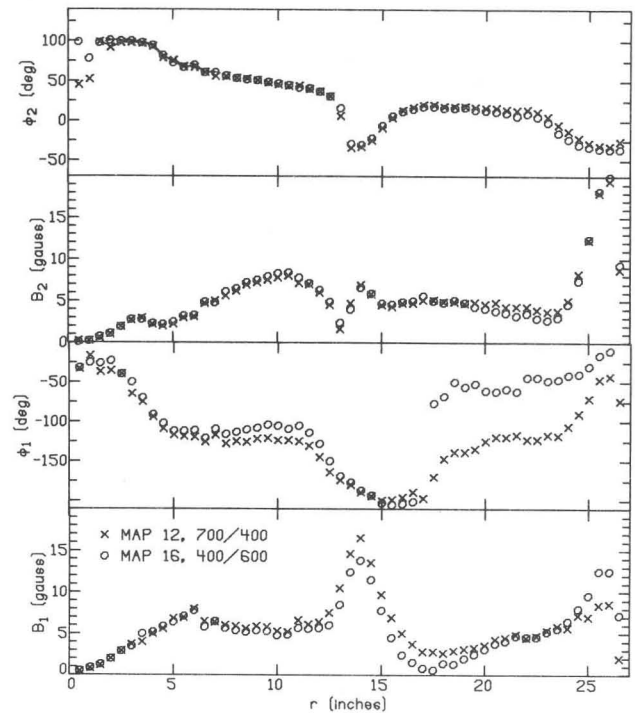


Fig. 5. Amplitude (B) and phase (ϕ) of first and second harmonics.

Conclusions

The magnet mapping apparatus produces field maps of high quality. They confirm the validity of a practical procedure for calculating the field in a saturated iron magnet. The first and second harmonics in the magnetic field are small, and we expect that some reduction of the amplitude can be achieved, at least for the first harmonic, by better alignment.

References

1. S.W. Mosko, E.D. Hudson, R.S. Lord, D.C. Hensley, and J.A. Biggerstaff, IEEE Transactions on Nuclear Science NS-24 (June 1977) 1269.
2. H.G. Blosser, D.A. Johnson, Field Calculations for the MSU 500 MeV Superconducting Magnet, MSU CP-28 (1977).